

OphNet: A Large-Scale Video Benchmark for Ophthalmic Surgical Workflow Understanding

Ming Hu^{1,2,3*}, Peng Xia^{1,3*}, Lin Wang^{4*}, Siyuan Yan¹, Feilong Tang^{1,3}
Zhongxing Xu⁶, Yimin Luo⁷, Kaimin Song^{1,3}, Jurgen Leitner²
Xuelian Cheng¹, Jun Cheng⁵, Chi Liu¹, Kaijing Zhou^{8†}, and Zongyuan Ge^{1,2,3†}

¹ AIM Lab, Faculty of IT, Monash University

² Faculty of Engineering, Monash University

³ Airdoc-Monash Research, Airdoc

⁴ Bosch (China) Investment Co. Ltd.

⁵ Institute for Infocomm Research, A*STAR

⁶ Weill Cornell Medicine, Cornell University

⁷ Division of Imaging Sciences and Biomedical Engineering, King's College London

⁸ National Clinical Research Center for Ocular Diseases, Wenzhou Medical University

Abstract. Surgical scene perception via videos are critical for advancing robotic surgery, telesurgery, and AI-assisted surgery, particularly in ophthalmology. However, the scarcity of diverse and richly annotated video datasets has hindered the development of intelligent systems for surgical workflow analysis. Existing datasets for surgical workflow analysis, which typically face challenges such as small scale, a lack of diversity in surgery and phase categories, and the absence of time-localized annotations, limit the requirements for action understanding and model generalization validation in complex and diverse real-world surgical scenarios. To address this gap, we introduce OphNet, a large-scale, expert-annotated video benchmark for ophthalmic surgical workflow understanding. OphNet features: 1) A diverse collection of 2,278 surgical videos spanning 66 types of cataract, glaucoma, and corneal surgeries, with detailed annotations for 102 unique surgical phases and 150 granular operations; 2) It offers sequential and hierarchical annotations for each surgery, phase, and operation, enabling comprehensive understanding and improved interpretability; 3) Moreover, OphNet provides time-localized annotations, facilitating temporal localization and prediction tasks within surgical workflows. With approximately 205 hours of surgical videos, OphNet is about 20 times larger than the largest existing surgical workflow analysis benchmark. Our dataset and code have been made available at: <https://github.com/minghu0830/OphNet-benchmark>.

Keywords: Surgical Workflow Understanding · Ophthalmic Surgery · Medical Image Analysis · Video Benchmark

* Equal contribution

† Corresponding author

1 Introduction

As surgical robot platforms such as the Da Vinci[®] Surgical System become increasingly sophisticated, there is growing interest in integrating enhanced intelligence into scenarios like minimally invasive surgery [22,38,78]. The advancements in machine vision perception empower these robotic systems to autonomously recognize and adapt to the intricacies of surgical environments, without relying on binary instrument usage signals, RFID tags, sensor data from tracking devices, or other signal information that necessitates laborious manual annotations or additional equipment installations [31]. This autonomy includes the capacity to identify anatomical structures, detect anomalies, and adjust surgical plans in real-time, which is crucial in dynamic and unpredictable surgical settings. In recent years, especially in endoscopy and ophthalmic surgery, the application of deep learning has demonstrated considerable promise in bolstering these autonomous capabilities. This encompasses the analysis of surgical workflows [6, 31, 84], segmentation of instruments and anatomy [4, 26, 50], and depth estimation [86], among others.

Automatic video surgical workflow understanding is a fundamental yet challenging problem for developing computer-assisted and robotic-assisted surgery, which can be divided into internal (e.g. laparoscopic and endoscopic [31, 54, 66]) and external (e.g. operating room and nursing procedure [48]) analysis. In addition to promoting the development of intelligent surgery, it also greatly benefits surgical documentation, education, and training [12, 13, 75]. Baret et al. [6] showed networks, like Inflated 3D ConvNet (I3D) [11] that utilize spatiotemporal convolutions, require a relatively extensive dataset for effective training. In their study, the model achieves an accuracy exceeding 80% when trained on 100 videos, with a progressive improvement as the sample size surpasses 700. However, the highly efficient and rapidly evolving deep learning technologies for surgical workflow analysis are currently limited by the following shortcomings in current video benchmarks: **1) Small scale:** the majority of video datasets contain no more than 100 videos. For example, the CATARACTS [25] and CatRelDet [25] datasets contain only 50 and 21 surgical videos, respectively. These datasets are relatively small, insufficient for large-scale validation. **2) Limited categories of surgeries and phases:** almost all ophthalmic surgical video datasets only include cataract surgery and do not further classify specific types of surgeries. Additionally, the number of phase categories is also limited, like CatRelDet [25] only contains 4 different phase labels, which is insufficient to meet the requirements for evaluation in real clinical environments. **3) Coarse-grained annotation:** due to annotation costs, existing benchmarks often have coarse-grained action definitions. For example, adhesive injection may occur in two different phases: main incision and capsulorhexis, so it may be classified into different phase categories. Coarse-grained action definitions may lead to annotation bias. **4) Single time-boundary annotation:** they only annotate designated phases in the videos, ignoring the continuity across different stages of ophthalmic surgery, as well as the hierarchical relationship between surgery, phase, and operation. Simpler datasets, such as LensID [24], are limited

Protocol	Dataset Properties						Tasks			
	Datasets	No. of Videos	No. of Action Segments	No. of Surgery Categories	No. of Action Categories	Total Duration	Multi-Surgery Presence Recognition	Phase Recognition	Phase Localization	Phase Prediction
Endo&Lap	Cholec120 [52]	120	-	1	7	76.2h	✗	✓	✗	✗
	SurgicalActions160 [63]	160	160	1	16	0.2h	✗	✓	✗	✗
	HeiCo [46, 58]	30	-	3	14	2.8h	✗	✓	✓	✓
	EndoVis 2021 [77]	33	250	1	7	22.0h	✗	✓	✗	✗
	PitVis [3]	25	287	1	17	33.3h	✗	✓	✗	✗
	CholecT50 [53]	50	-	1	10	44.7h	✗	✓	✓	✓
	AutoLaparo [80]	21	300	1	7	23.1h	✗	✓	✓	✓
OphScope	LensID [24]	100	2,440	1	2	11.7h	✗	✓	✗	✗
	Cataract-101 [64]	101	1,266	1	10	14.0h	✗	✓	✓	✓
	CatRelDet [25]	21	2,400	1	4	2.0h	✗	✓	✗	✗
	CATARACTS [4]	50	1,536	1	19	20.0h	✗	✓	✓	✓
	OphNet (Ours)	2,078	9,795	66	150	204.8h	✓	✓	✓	✓

Table 1: The statistics comparison among existing workflow analysis datasets and our OphNet. Compared to other datasets, OphNet focuses on more comprehensive coverage of various surgery, phase and operation categories, collects a large number of videos, totaling 204.8 hours, and also enables a variety of recognition, localization and prediction tasks. OphNet demonstrates considerable competitiveness in both its scale and the richness of its labels. *Endo&Lap* denotes the endoscopic and laparoscopic protocol, *OphScope* denotes the ophthalmic microscope protocol. We choose the latest version for comparison in cases where datasets have multiple supplementary updates. For instance, Cholec120 [52], Cholec80 [75], m2cai-workflow and LapChole [71] form one series, whereas CholecT50 [53], CholecT45 [53], and CholecT40 [51] comprise another series. We have excluded the following scenarios from our comparison: (1) non-open-source datasets such as Bypass170 [76], ESD [35], Yu’s [84], etc.; (2) a superset of multiple open-source or non-open-source datasets, like Cholec207 [6], etc.; (3) datasets employed for lesion, anatomy, and instrument classification and segmentation, such as SUN-SEG [30], CVC-ClinicDB [7], ROBUST-MIS [61], Mesejo’s [47], Cata7 [50], etc., anomaly detection such as PolypDiag [73] (from Hyper-Kvasir [9] and LDPolypVideo [45]), Kvasir-Capsule [68], etc., and other datasets not dedicated to workflow analysis. It’s worth mentioning that even in comparison with the above datasets, OphNet demonstrates considerable competitiveness in both its scale and the richness of its labels.

to binary classification tasks distinguishing lens implantation from other irrelevant phases. **5) Uniform domain:** the videos are meticulously collected, and while this ensures video quality, the uniform style is not conducive to testing the model’s domain generalization ability.

While some works have explored semi-supervised and self-supervised learning strategies [8, 59, 83, 85] to alleviate the cost of annotations or use only a small fraction of available labels, these approaches still lack competitiveness in performance compared to fully supervised learning. This deficiency in performance is impeding the widespread clinical application of these strategies. To address the shortage of sufficient labeled datasets, we construct OphNet, a large-scale

and expert-level video benchmark with high diversity, for ophthalmic surgical workflow understanding. The main advantages of OphNet are as follows:

- **Largest scale and diversity:** to the best of our knowledge, OphNet is currently the largest and most richly labeled dataset for surgical workflow analysis. It contains a number of videos 20 times greater than the current largest benchmark in ophthalmic surgery and far exceeds datasets in more established fields such as endoscopy. Additionally, OphNet includes the greatest variety of different types of surgeries, encompassing 66 different surgeries such as cataract, glaucoma, and corneal surgeries, along with 102 unique surgical phases and 150 distinct operations. This diversity significantly surpasses that of previous research.
- **Fine-grained, sequential and hierarchical annotation:** we have meticulously selected a subset of videos for annotation localization, with each video being marked for an average of 13 phases and 17 operations. Additionally, we provide exquisite annotations at the levels of surgery, phase, and operation, catering to the requirements for training specific challenge models. This annotation design aims to offer a multifaceted understanding of surgical protocols, accommodate the nuances of each distinct surgery, and enhance the usability and interpretability of our dataset.
- **Expert-level manual annotation:** the annotation work for OphNet was completed by ten experienced ophthalmologists and five individuals with ophthalmic experience, encompassing, but not limited to, standardization of definitions for surgery, phase, and operation labels, video filtering, classification and localization annotations, and secondary verification, among others. Expert-level annotators ensure the quality and professionalism of OphNet.

2 Related Work

Surgical Workflow Understanding. Beyond its therapeutic advantages, minimally invasive surgery also provides the capability for operative video recording. These videos can be stored and later utilized for various purposes such as cognitive training, skill assessment, and surgical workflow analysis. Techniques derived from the broader field of video content analysis and representation are increasingly being incorporated into the surgical realm [6, 43, 84]. A typical surgical workflow can be defined by a sequence of tasks or events, including patient positioning, incision, dissection, and suturing. These events are influenced not only by the specific type of surgery but also by the individual surgeon’s proficiency and technique. Consequently, a comprehensive understanding of the surgical workflow necessitates a thorough examination of the temporal, spatial, and contextual facets of these tasks.

Weakly-Supervised Video Learning. Substantial pioneering work has been undertaken in the realms of video understanding [5, 18, 39, 62, 79, 81, 82, 87]. Since even a small amount of videos easily comprises several million frames, methods that do not rely on a frame-level annotation are of special importance. Weakly-supervised video learning makes use of loosely labeled data to train models,

thereby obviating the necessity for exhaustively annotated training data. These weak labels might manifest in a variety of forms, including video-level labels or partial labels, which are less specific than frame-level or pixel-level annotations. The objective of weakly-supervised learning is to utilize these coarse labels to produce models capable of delivering fine-grained predictions, such as temporally precise action localization or detailed semantic segmentation [17, 42]. The large-scale annotation of surgical videos demands a significant investment of invaluable medical time resources. In this context, weakly supervised learning emerges as a viable solution to this bottleneck.

Action Anticipation. Action anticipation involves predicting future actions having observed the initial portion of a video. Typically, the observed video is processed as a whole to obtain a video-level representation of the ongoing activity in the video, which is then used for future prediction [33, 34]. Existing anticipation tasks can be grouped into two categories based on the anticipation duration: 1) near-term action anticipation [14, 37] involves predicting label for the immediate next action that would occur in the range of a few seconds having observed a short video segment of duration of a few seconds, and 2) long-term action anticipation [60] needs to exploit temporal dependencies among observed actions to generate plausible human action sequences in the long-term. Action anticipation is an important task in computer vision field with many applications [10]. The task of predicting actions is of immense relevance across a variety of applications, such as comprehending human-object and human-human interaction [23, 89], accident prediction [72], and road traffic understanding [28, 40]. Surgical action anticipation is a valuable tool that can greatly assist surgeons in their decision-making process [51, 55].

3 Dataset Construction

In this section, We describe the construction of the dataset involved meticulous data collection and preprocessing, leveraging YouTube as a primary source to circumvent privacy issues while ensuring a broad representation of ophthalmic surgeries. The selection criteria aimed at capturing a wide array of video qualities and styles, specifically targeting cataract, glaucoma, and corneal surgeries due to their prevalence in clinical settings. Efforts were made to refine the dataset by excluding videos of inadequate quality or those depicting non-human subjects. The annotation process was structured to reflect the complex nature of eye surgeries, incorporating hierarchical classification to account for the multiple conditions often treated within a single procedure. This was complemented by detailed localization annotations, delineating the distinct phases and techniques characteristic of ophthalmic operations, undertaken by a dedicated team of ophthalmologists to ensure accuracy and relevance.

3.1 Data Collection & Preprocessing

Collection. Medical data exhibit unique privacy considerations and tend to be of smaller data volumes, characteristics that are particularly salient in the

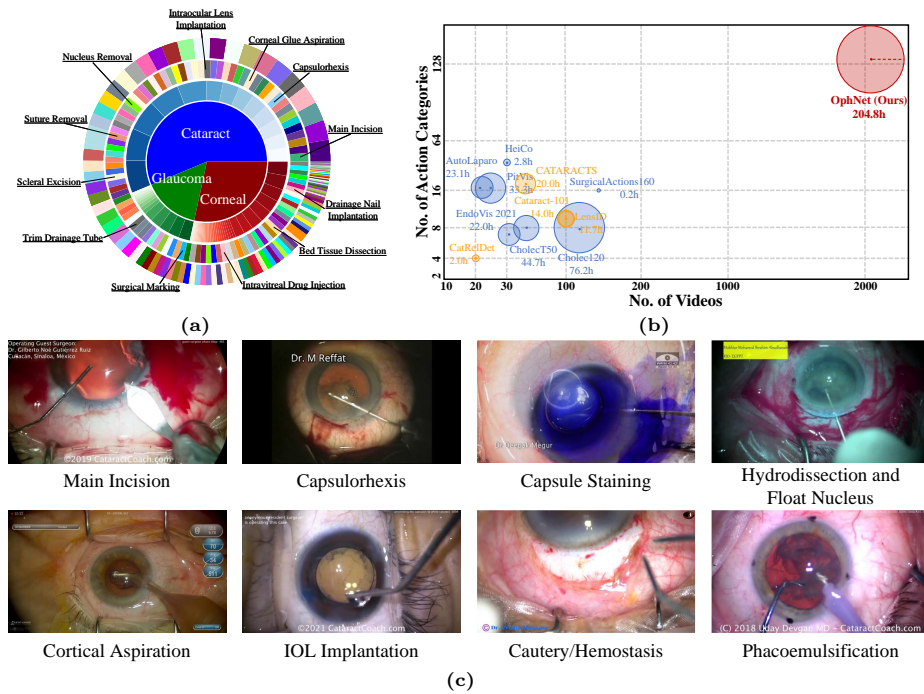


Fig. 1: OphNet’s composition, comparison with other datasets for the same task, and some phase examples: (a) an overview of the composition ratios at the levels of surgery, phase, and operation; (b) comparison among existing open-source \bullet laparoscopic & endoscopic, and \circ ophthalmic microscope workflow analysis video datasets and \bullet our OphNet. OphNet stands as the largest real-world video dataset for ophthalmic surgical workflow understanding, featuring the highest number of videos, longest duration, and diverse categories of surgeries and phases; (c) eight phase examples in OphNet.

case of video data. By capitalizing on the wealth of surgical videos available on YouTube, we are able to obviate potential ethical and privacy concerns while concurrently enabling the rapid procurement of a substantial corpus of videos for further screening [1, 2, 19, 32]. To fulfill this objective, we deploy text-based search algorithms to probe each surgery on YouTube, obtaining videos with titles that incorporate the requisite surgical keywords. We select cataract, glaucoma, and corneal surgery—three of the most commonly performed ophthalmic surgeries in actual clinical environments—as the central subjects of our research. To expand our video collection, we bolster our search queries by integrating synonyms and abbreviations associated with each type of ophthalmic surgery. For instance, *cataract surgery* encompasses various types: *Phacoemulsification* (abbr. PHACO), *Intraocular Lens implantation* (abbr. IOL), and *Extracapsular Cataract Extraction* (abbr. ECCE), etc.

Preprocessing. Given the nature of text-based retrieval and the varying quality, style, and filming methods of surgical videos influenced by different YouTube sources, some videos may exhibit poor quality or deviations in surgical represen-

tation. We filter out low-resolution videos, black-and-white color schemes, and animated demonstrations. Furthermore, surgical videos featuring non-human eyes, such as pig eyes, rabbit eyes, or pseudo-human eyes, are also outside the scope of our annotation. The data preprocessing was jointly completed by five professionals with experience in ophthalmology for initial screening, followed by a review conducted by six attending ophthalmologists.

3.2 Data Annotation

Hierarchical Classification Annotation. Different from the single-label classification in most natural video datasets [19, 27, 67, 69, 90], in ophthalmic surgery, physicians typically consider and implement multiple types of surgeries and phases based on the specific conditions and needs of the patient. This multifaceted approach stems from the complexity of the eye as an organ, where numerous diseases often coexist. Consequently, multiple ocular problems may need to be addressed in a single surgery. As shown in Fig. 2, a patient with cataracts may also have glaucoma, necessitating the simultaneous treatment of both conditions within one surgery. Hence, we initially classified all videos based on the primary surgical categories into three principal groups: cataract, glaucoma, and corneal surgeries. Subsequently, these were further allocated for the detailed annotation of primary and secondary surgery. It is important to note that there exists only a single type of primary surgery, whereas multiple secondary surgery may be present. The categorization and annotation were meticulously completed by a team comprised of 8 experienced ophthalmologists.

Localization Annotation. A single surgery is often multifaceted, involving a series of intricate phases, each requiring distinct techniques and instruments, and the transition between surgeries entails high precision and coordination. Routine cataract surgery involves several steps. It begins with the administration of anesthesia, followed by a small incision in the cornea. The surgeon then creates an opening in the lens capsule and uses ultrasonic vibrations to break up and remove the cataract. Afterward, an artificial intraocular lens (IOL) is inserted into the lens capsule, and the incision is sealed without stitches. We define the phases and operation for various surgeries based on the textbook *Ophthalmic Surgery: Principles and Practice* [70]. To ensure the quality of localization annotations, we assign each annotator videos of 2-6 different types of secondary surgeries. This process resulted in a minimum of three annotated action boundaries for each video. We also employed the complete linkage algorithm [15] to cluster and merge various temporal boundaries into stable boundaries that received multiple agreements. It's worth noting that an individual video may have multiple separate instances of the same or different phases, thereby leading to multiple boundary definitions. A team of 15 ophthalmologists completes the localization annotation.

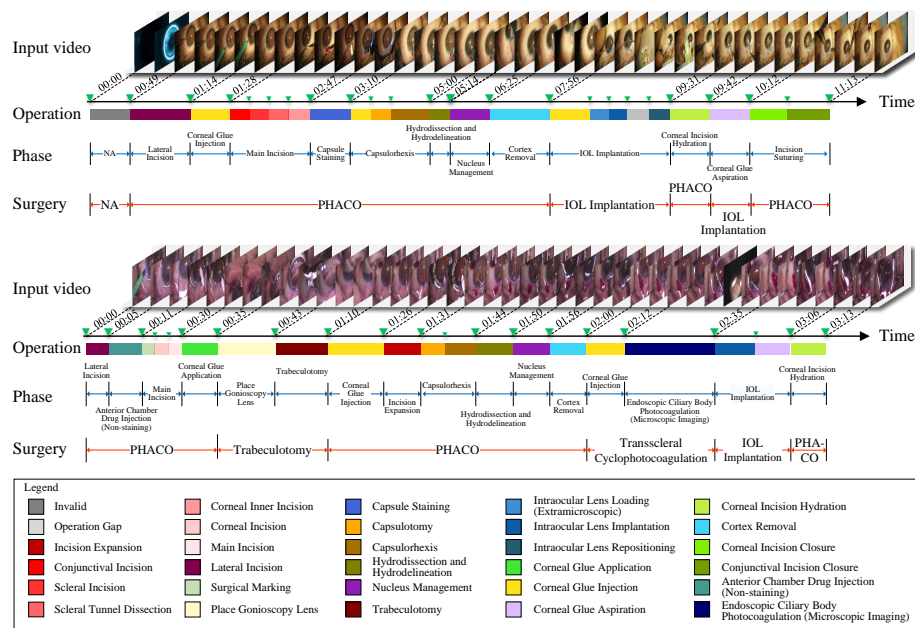


Fig. 2: The figure shows two combined surgical videos, *PHACO + IOL implantation* and *PHACO + Trabeculotomy + Transscleral Cyclophotocoagulation + IOL implantation*. For each frame marked in color, we provide time-boundary annotations at surgical, phase and operation levels.

3.3 Dataset Statistics and Analysis

OphNet includes 2,078 surgical videos (204.8 hours), demonstrating 66 different types of ophthalmic surgeries: 13 types of cataract surgery, 14 types of glaucoma surgery, and 39 types of corneal surgery. There are 102 phases and 150 operations for recognition, detection and prediction tasks, summarized in Tab. 1. Over 77% of videos have high-definition resolutions of 1280 x 720 pixels or higher. To facilitate algorithm development and evaluation, we selected 523 videos for localization annotations. Additionally, we trim videos according to annotated action boundaries, resulting in 7,320 phase instances and 9,795 operation instances, totaling 51.2 hours. The average duration of trimmed videos is 32 seconds, while untrimmed videos average 337 seconds.

4 Experiments

In our study, we explore four potential tasks using the OphNet dataset: 1) surgery presence recognition, 2) phase and operation recognition, 3) phase localization, and 4) phase anticipation. To establish robust baselines, we employ state-of-the-art models known for their effectiveness in human action recognition, detection and anticipation. For each task, we provide a detailed problem formulation and evaluate the baseline models' performance. Our findings offer valuable insights

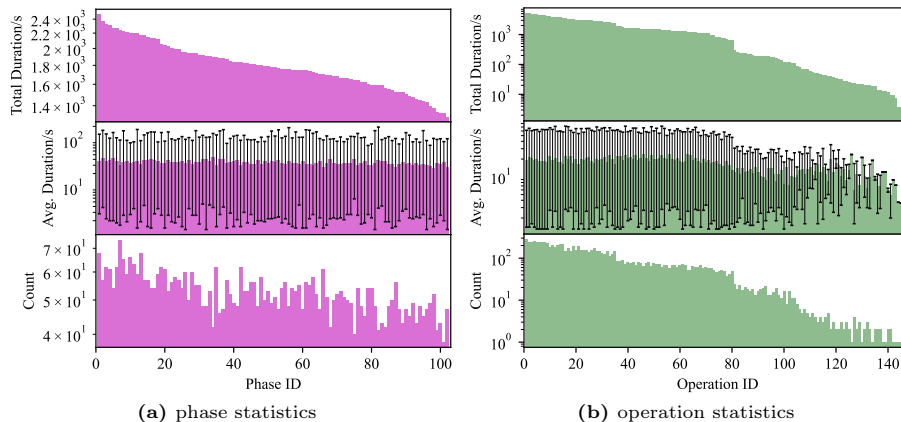


Fig. 3: We present the data statistics of trimmed videos at the levels of phase and operation, including the number of trimmed videos, average duration, and total duration. The IDs and corresponding names can be found in the appendix.

into video understanding within sequences and fine granularity, contributing to the field’s knowledge of video tasks in medical contexts.

4.1 Surgery Presence, Phase and Operation Recognition

Task Description. Surgery presence recognition focuses on identifying various surgical types in untrimmed videos through weakly supervised methods. This requires the model to discern and capture distinct surgical action features within extensive video footage. In OphNet, every surgical procedure within each video is annotated. We identify the primary surgery based on the key objectives and durations of the surgeries. To streamline the process, our experiments are limited to recognizing the presence of these primary surgeries. Additionally, phase recognition segments the surgery into distinct phases using visual cues and movements, such as incision, lens removal, and implantation. Meanwhile, operation recognition involves identifying finer-grained surgical actions.

Setup. For the surgery presence recognition experiment, we simplified the process and only considered the presence of the primary surgery in untrimmed videos. The dataset was randomly partitioned to ensure a balanced representation of examples for each surgery category. Specifically, we allocated 70% of the data for training (1,449 surgical videos), 10% for validation (205 surgical videos), and 20% for testing (424 surgical videos). For the phase and operation recognition experiments, we maintained the same settings, with 70% of the data used for training (5,024 phase segments, 6,856 operations segments), 10% for validation (730 phase segments, 975 operations segments), and 20% for testing (1,566 phase segments, 1,964 operations segments). The input for the surgery presence recognition experiment is untrimmed videos, while for the phase and operation recognition experiments, the input consists of trimmed segments. In all classification experiments, we set up the analysis and comparison from four

perspectives: cataract surgery, glaucoma surgery, corneal surgery, and all surgical videos.

Baselins. We compare the performance of I3D [11], SlowFast [21], X3D [20], and MViT V2 [36] models on this task. These models are evaluated in two versions: 1) random initialization training and 2) pre-training with weights from Kinetics 400 [32], which is a human action recognition dataset. In addition, we also explored the classification performance of X-CLIP [49] and ViFi-CLIP [57], two CLIP [56]-based models. We also compared the effects of different numbers of input frames on the models' performance, where the subscript "_16" represents an input of 16 frames, and "_32" represents an input of 32 frames.

Results. We summarize the results in Tab. 2 and Tab. 3. In primary surgery classification, X-CLIP [49] achieved the highest overall Top-1 accuracy at 58.9%, leading in cataract and glaucoma surgeries with accuracies of 60.6% and 53.5% respectively. For corneal surgeries, X-CLIP also recorded the highest Top-1 and Top-5 accuracies of 61.4% and 88.6%. In phase classification, ViFi-CLIP [57] led with the highest Top-1 accuracy, particularly in cataract surgeries at 75.9%, and exhibited the best performance in both glaucoma and corneal surgeries. Furthermore, in operation classification, ViFi-CLIP outperformed all other models in all categories, especially noted in cataract and corneal surgeries with Top-1 accuracies of 75.1% and 83.7% and Top-5 accuracies of 93.8% and 85.2% respectively. Overall, ViFi-CLIP showed superior performance in both phase and operation classifications across various surgery types. Besides, in the phase and operation classification experiments, a higher number of input frames generally had a positive effect on the model. In Fig. 4, we present the heatmap visualization of four examples from the test set of phase recognition experiments using the ViFi-CLIP model. It can be observed that in a series of frame images, the model focuses on surgical instruments and the operated eye area, which is consistent with human experience. The instruments used in the same phase of ophthalmic surgery are often similar.

4.2 Phase Localization

Task Description. Phase Localization in ophthalmic surgical workflow analysis refers to the task of pinpointing the exact moments or time intervals within a surgical video where specific phases of the surgery begin and end. This involves

Baselines	Primary Surgery Classification							
	Cataract		Glaucoma		Cornea		All	
	Top-1	Top-5	Top-1	Top-5	Top-1	Top-5	Top-1	Top-5
I3D [11]	38.9	86.3	43.6	71.7	42.7	78.2	29.8	53.2
SlowFast [21]	45.3	82.1	44.6	72.3	45.5	77.3	27.2	54.4
X3D [36]	42.1	87.4	44.6	74.2	43.8	76.6	28.5	62.7
MViT V2 [20]	43.2	84.2	45.5	81.8	45.5	75.9	29.1	60.1
I3D*	36.8	84.7	48.2	81.8	48.6	76.5	27.2	50.6
SlowFast*	49.0	83.7	47.3	80.9	49.2	75.6	27.2	50.6
X3D*	47.4	86.3	46.4	81.5	48.3	78.2	35.4	61.4
MViT V2*	44.2	85.3	49.1	81.8	47.7	77.3	28.5	63.3
X-CLIP ₁₆ [49]	58.5	94.7	51.8	92.8	61.4	88.6	40.5	79.0
X-CLIP ₃₂	60.6	92.6	53.5	83.7	56.8	84.1	58.9	81.0
ViFi-CLIP ₁₆ [57]	59.6	88.3	52.4	80.2	61.4	81.8	58.9	79.8
ViFi-CLIP ₃₂	59.6	88.3	51.5	84.8	50.0	75.0	56.3	77.2

Table 2: Per-class Top-1 and Top-5 accuracy (%) for the primary surgery presence recognition on untrimmed videos. The best performance for each split has been highlighted in **bold**.

Baselines	Phase Classification								Operation Classification							
	Cataract		Glaucoma		Cornea		All		Cataract		Glaucoma		Cornea		All	
	Top-1	Top-5	Top-1	Top-5	Top-1	Top-5	Top-1	Top-5	Top-1	Top-5	Top-1	Top-5	Top-1	Top-5	Top-1	Top-5
I3D [11]	27.2	55.7	24.1	57.5	18.9	52.1	25.7	58.2	26.8	54.9	23.5	56.0	18.0	51.2	25.0	57.1
SlowFast [21]	26.5	56.5	23.1	56.5	24.2	49.1	26.7	60.1	25.8	55.2	22.9	45.9	23.5	48.5	26.0	59.0
X3D [36]	27.0	58.3	21.0	55.5	21.8	28.5	26.6	62.3	26.4	47.2	20.5	44.6	21.3	27.8	26.1	61.5
MViT V2 [20]	26.2	54.9	21.0	53.4	26.0	46.8	27.0	59.8	25.9	43.8	20.5	42.7	25.5	45.9	26.5	58.9
I3D*	29.5	68.9	22.1	58.6	26.0	50.9	30.2	71.2	28.8	67.5	21.8	47.9	25.7	50.3	29.5	60.0
SlowFast*	30.6	72.3	25.2	54.7	30.7	59.8	31.7	61.8	29.9	71.1	24.8	43.9	29.5	58.7	30.5	60.9
X3D*	27.2	72.9	22.1	59.6	30.7	61.5	33.5	63.2	26.5	71.8	21.7	48.8	29.9	60.2	32.8	62.1
MViT V2*	34.2	76.5	23.3	52.0	38.4	65.1	28.3	60.2	33.5	75.2	22.8	41.5	37.9	64.0	27.8	59.5
X-CLIP ₁₆ [49]	68.3	92.2	47.3	89.8	53.0	77.4	63.4	85.3	67.5	91.0	46.5	78.9	82.2	76.1	62.5	84.0
X-CLIP ₃₂	69.1	94.0	48.7	81.7	54.8	80.4	62.7	85.8	68.0	93.0	47.9	80.5	84.0	79.5	62.0	84.7
ViFi-CLIP ₁₆ [57]	75.9	93.7	40.4	85.4	66.6	81.6	66.1	88.4	74.5	92.5	42.8	74.5	85.0	80.5	65.0	87.5
ViFi-CLIP ₃₂	73.0	92.9	49.6	82.7	57.7	81.6	68.4	87.2	75.1	93.8	43.2	80.2	83.7	85.2	64.8	86.5

Table 3: Per-class Top-1 and Top-5 accuracy (%) for the primary surgery presence recognition on untrimmed videos and phase recognition on trimmed videos. * denotes the initialization from the model pre-trained on Kinetics 400 [32]. For the two CLIP models, we chose ViT-B/16 as the backbone and compared the performance of two different input frame numbers, 16 and 32. The best performance for each split has been highlighted in **bold**.

Baselines	Backbones	mAP (%)					Baselines	Top-1 Acc. (%)				
		0.1	0.3	0.5	0.7	Avg.		0.1	0.3	0.5	0.7	Avg.
ActionFormer [87]	CSN [74]	53.7	50.1	40.6	24.5	42.5	I3D [11]	26.5	42.2	49.8	51.3	47.3
	SwinVivIT [41]	59.3	54.7	43.3	26.3	46.4	SlowFast [21]	25.4	42.6	48.9	52.2	47.2
	SlowFast [21]	60.0	55.9	45.1	26.0	47.5	MViT V2 [20]	25.6	43.7	49.3	52.3	47.5
TriDet [65]	CSN	56.1	53.0	43.1	29.4	46.2	I3D*	27.3	43.5	50.1	51.4	47.6
	SwinVivIT	61.0	57.1	47.1	33.1	50.4	SlowFast*	27.5	43.2	49.9	52.3	47.8
	SlowFast	61.3	56.0	45.6	30.4	48.6	MViT V2*	27.8	44.3	85.0	51.7	48.2

Table 4: The results for phase detection. ActionFormer and TriDet are state-of-the-art models for anticipation. We report top-1 accuracy at the observation ratios [0.1:0.2:0.9]. Average top-1 accuracy is computed by averaging different IoU thresholds. The best performance for each split has been highlighted in **bold**.

Table 5: The results for phase detection. We report top-1 accuracy at the observation ratios [0.1:0.2:0.9]. Average top-1 accuracy is computed by averaging different IoU thresholds. The best performance for each split has been highlighted in **bold**.

the detailed temporal segmentation of the entire surgical procedure into its constituent phases based on visual cues, surgeon’s actions, and the progression of the surgery. The objective of phase localization is to accurately identify the start and end times of different surgical stages, such as pre-operative preparation, incision, and removal of the lens facilitating a granular and precise understanding of the surgery timeline. This task is crucial for detailed surgical documentation, efficient surgical training, and the development of targeted interventions during specific stages of the surgery, enhancing overall surgical management and post-operative analysis.

Setup. We excluded *Operation Gap* and *Invalid*, and filtered out tags with fewer than 20 segments. We used two baseline models, ActionFormer [87] and TriDet [65], with backbone networks configured as CSN [74], SwinVivIT [41], and SlowFast [21]. To extract features from the videos, we first extracted RGB

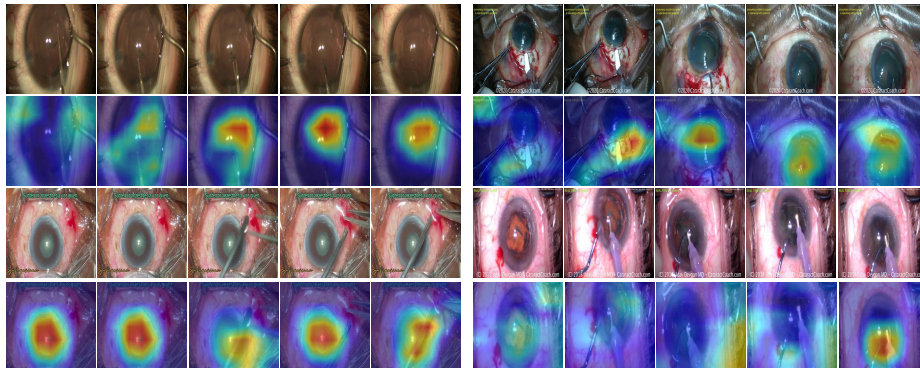


Fig. 4: Attention map visualizations of ViFi-CLIP [57] on four examples from OphNet test set in the phase recognition task.

frames from each video at a rate of 25 frames per second. We also extracted optical flow using the TV-L1 [29, 44] algorithm. We then fine-tuned an I3D [11] model that had been pre-trained on the ImageNet [16] dataset, and used it to generate features for each RGB and optical flow frame. Because each video has a variable duration, we performed uniform interpolation to generate 100 fixed-length features for each video. Finally, we concatenated the RGB and optical flow features into a 2048-dimensional embedding, which served as the input for our model.

Baselins. We conducted the experiments using phase-level labels and used two baseline models, ActionFormer [87] and TriDet [65], with backbone networks configured as CSN [74], SwinViviT [41], and SlowFast [21]. Data split follows the setup of the primary surgery classification experiment.

Results. The experimental results for phase localization are presented in the Tab. 4, showcasing the performance of different baseline models with various backbones in terms of mean Average Precision (mAP) at different Intersection over Union (IoU) thresholds [0.1:0.2:0.9]. The models evaluated include ActionFormer with SwinViviT and SlowFast backbones, and TriDet with CSN, SwinViviT, and SlowFast backbones. The results indicate that the TriDet model with a SwinViviT backbone outperforms other combinations, achieving the highest mAP scores across most IoU thresholds, with notable scores of 61.0% (IoU=0.1), 57.1% (IoU=0.3), 47.1% (IoU=0.5), and 33.1% (IoU=0.7), resulting in an average mAP of 50.4%. This indicates that the TriDet model, especially when combined with the SwinViviT backbone, is particularly effective for phase localization in surgical videos. On the other hand, the TriDet model with a SlowFast backbone shows competitive performance, particularly achieving the highest mAP of 61.3% at the lowest IoU threshold (0.1). However, it falls slightly behind in performance at higher IoU thresholds compared to the SwinViviT backbone.

4.3 Phase Anticipation

Task Description. This task requires the analysis of real-time or recorded video data to foresee the sequence of events based on current and past surgical

activities. By understanding the typical progression of ophthalmic surgeries and recognizing patterns in the surgeon’s actions and the use of instruments, the system aims to forecast the next phase of the surgery, allowing for proactive preparation and response. The objective of phase anticipation is to enhance the efficiency and safety of surgical procedures by providing the surgical team with advanced notice of upcoming steps, enabling better resource allocation, timing for critical tasks, and overall coordination within the operating room.

Setup. Following previous approaches of the primary surgery classification experiment in Sec. 4.1, We randomly mask phase sequences in the test video with different observation ratios.

Baselins. We evaluate our datasets with the baseline models such as I3D [11], SlowFast [21], and MViT V2 [36]. For each model, we also adopted two training approaches: random initialization training and using pre-trained weights from Kinetics 400 [32].

Results. We show the phase detection results in Tab. 5. The results demonstrate that the baseline models pretrained on Kinetics 400 [32] generally outperform their original counterparts in terms of Top-1 accuracy across different observation ratios for phase anticipation. Specifically, the modified MViT V2* model exhibits the highest improvement, achieving the best average Top-1 accuracy of 48.2%. Moreover, while all models show increased accuracy with higher observation ratios, indicating that more observed data contributes to better performance, the consistent improvement across all ratios for the enhanced models suggests effective modifications.

5 Limitations

Dataset Bias. OphNet’s videos are sourced from YouTube and exhibit diverse styles, clarity, and screen elements. This diversity can aid detection models in generalization but may affect their effectiveness and performance. Some videos in the dataset include subtitles or additional video windows, such as watermark shown in Fig. 1. Similarly, additional video windows offer another perspective but can make the scene chaotic, making it harder to recognize primary surgical actions. The presence of these factors in OphNet reflects the complexity of real-world surgical environments, because an ophthalmic microscope may inherently display different windows or show parameters during recording. While they pose challenges, they also present opportunities for developing models that can better handle variability and unpredictability, which are crucial aspects of real-world surgical scenarios.

Annotation Bias. OphNet is entirely annotated by ophthalmologists, there is a distinct possibility of annotation bias reflecting specific regional practices, terminologies, and interpretations. Despite the universal nature of many ophthalmic procedures, subtle differences in surgical techniques, procedural preferences, and clinical terminologies could lead to inconsistencies in how surgeries are categorized and described across different regions. For instance, the terminology used to describe certain procedures might differ, with one region referring to a pro-

cedure as "anterior vitrectomy" while another uses "pars plana vitrectomy." To reduce the possibility of biases in precise annotations, we have taken great care to establish a unified definition prior to describing the surgery, phase and operation. However, potential biases arising from regional variations and individual surgical practices are inevitable.

Long-tailed Distribution. The skewed distribution observed in OphNet is consistent with real-world healthcare scenarios. Typically, certain types of surgeries and procedures are more common due to prevalent conditions and diseases. For instance, cataract surgeries are performed more frequently worldwide than more complex vitreoretinal surgeries. This prevalence is reflected in the data, contributing to the skewness where a few surgery types dominate (the head), while many other types are rare occurrences (the tail). Given this understanding, it is crucial to recognize the skewed distribution in OphNet as an inherent characteristic of medical data rather than a flaw.

6 Conclusion

In response to the current challenges in ophthalmology, a surgical field apt for automation and remote control, we have introduced OphNet, a large-scale, diverse, and expert-level video benchmark for understanding ophthalmic surgical workflows. OphNet is the most extensive dataset of its kind, containing a broad range of cataract, glaucoma, and corneal surgeries and detailed annotations for distinct surgical phases. OphNet comprises 2,078 surgical videos (204.8 hours), 7,320 phase segments and 9,795 operation segments (51.2 hours), spanning 204.8 hours, showcasing 66 different types of ophthalmic surgeries: 13 cataract, 14 glaucoma, and 39 corneal. It is annotated with 102 phases and 150 operations. With OphNet, we explored primary surgery presence recognition, phase localization and phase anticipation on untrimmed videos, phase and operation recognition on trimmed videos. We employed state-of-the-art models to establish robust baselines and provided valuable insights into video understanding within sequences and fine granularity. Our work contributes to the broader understanding of surgical video tasks in medical contexts and promotes the integration of deep learning technologies into ophthalmic surgical procedures.

References

1. Fair use on youtube. <https://support.google.com/youtube/answer/9783148?hl=en#:~:text=If%20the%20use%20of%20copyright,copyright%20removal%20request%20to%20YouTube.>
2. Youtube's copyright exception policy. <https://www.youtube.com/howyoutubeworks/policies/copyright/#copyright-exceptions>
3. Adrito, D., Danyal, Z.K., Dimitrios, P., Yitong, Z., John, G.H., Francisco, V., Sophia, B., Hani, J.M., Danail, S.: Pitvis: Workflow recognition in endoscopic pituitary surgery

4. Al Hajj, H., Lamard, M., Conze, P.H., Roychowdhury, S., Hu, X., Maršalkaitė, G., Zisimopoulos, O., Dedmari, M.A., Zhao, F., Prellberg, J., Sahu, M., Galdran, A., Araújo, T., Vo, D.M., Panda, C., Dahiya, N., Kondo, S., Bian, Z., Vahdat, A., Bialopetravičius, J., Flouty, E., Qiu, C., Dill, S., Mukhopadhyay, A., Costa, P., Aresta, G., Ramamurthy, S., Lee, S.W., Campilho, A., Zachow, S., Xia, S., Conjeti, S., Stoyanov, D., Armaitis, J., Heng, P.A., Macready, W.G., Cochener, B., Quellec, G.: Cataracts: Challenge on automatic tool annotation for cataract surgery. *Medical Image Analysis* **52**, 24–41 (2019). <https://doi.org/https://doi.org/10.1016/j.media.2018.11.008>, <https://www.sciencedirect.com/science/article/pii/S136184151830865X>
5. Alwassel, H., Giancola, S., Ghanem, B.: TSP: Temporally-sensitive pretraining of video encoders for localization tasks. In: *Proceedings of the IEEE/CVF International Conference on Computer Vision Workshops*. pp. 3173–3183 (2021)
6. Bar, O., Neimark, D., Zohar, M., Hager, G.D., Girshick, R., Fried, G.M., Wolf, T., Asselmann, D.: Impact of data on generalization of ai for surgical intelligence applications. *Scientific Reports* **10**(1), 22208 (Dec 2020). <https://doi.org/10.1038/s41598-020-79173-6>, <https://doi.org/10.1038/s41598-020-79173-6>
7. Bernal, J., Sánchez, F.J., Fernández-Esparrach, G., Gil, D., Rodríguez, C., Vilarinho, F.: Wm-dova maps for accurate polyp highlighting in colonoscopy: Validation vs. saliency maps from physicians. *Computerized Medical Imaging and Graphics* **43**, 99–111 (2015). <https://doi.org/https://doi.org/10.1016/j.compmedimag.2015.02.007>, <https://www.sciencedirect.com/science/article/pii/S0895611115000567>
8. Bodenstedt, S., Wagner, M., Katić, D., Mietkowski, P., Mayer, B., Kenngott, H., Müller-Stich, B., Dillmann, R., Speidel, S.: Unsupervised temporal context learning using convolutional neural networks for laparoscopic workflow analysis. *arXiv preprint arXiv:1702.03684* (2017)
9. Borgli, H., Thambawita, V., Smedsrud, P.H., Hicks, S., Jha, D., Eskeland, S.L., Randel, K.R., Pogorelov, K., Lux, M., Nguyen, D.T.D., Johansen, D., Griwodz, C., Stensland, H.K., Garcia-Ceja, E., Schmidt, P.T., Hammer, H.L., Riegler, M.A., Halvorsen, P., de Lange, T.: HyperKvasir, a comprehensive multi-class image and video dataset for gastrointestinal endoscopy. *Scientific Data* **7**(1), 283 (2020). <https://doi.org/10.1038/s41597-020-00622-y>, <https://doi.org/10.1038/s41597-020-00622-y>
10. Cai, Y., Li, H., Hu, J.F., Zheng, W.S.: Action knowledge transfer for action prediction with partial videos. *Proceedings of the AAAI Conference on Artificial Intelligence* **33**(01), 8118–8125 (Jul 2019). <https://doi.org/10.1609/aaai.v33i01.33018118>, <https://ojs.aaai.org/index.php/AAAI/article/view/4820>
11. Carreira, J., Zisserman, A.: Quo vadis, action recognition? a new model and the kinetics dataset. In: *proceedings of the IEEE Conference on Computer Vision and Pattern Recognition*. pp. 6299–6308 (2017)
12. Czempiel, T., Paschali, M., Keicher, M., Simson, W., Feussner, H., Kim, S.T., Navab, N.: Tecno: Surgical phase recognition with multi-stage temporal convolutional networks. In: Martel, A.L., Abolmaesumi, P., Stoyanov, D., Mateus, D., Zuluaga, M.A., Zhou, S.K., Racoceanu, D., Joskowicz, L. (eds.) *Medical Image Computing and Computer Assisted Intervention – MICCAI 2020*. pp. 343–352. Springer International Publishing, Cham (2020)
13. Czempiel, T., Paschali, M., Ostler, D., Kim, S.T., Busam, B., Navab, N.: Opera: Attention-regularized transformers for surgical phase recognition. In: *Medical Image Computing and Computer Assisted Intervention–MICCAI 2021: 24th Interna-*

- tional Conference, Strasbourg, France, September 27–October 1, 2021, Proceedings, Part IV 24. pp. 604–614. Springer (2021)
14. Damen, D., Doughty, H., Farinella, G.M., Fidler, S., Furnari, A., Kazakos, E., Moltisanti, D., Munro, J., Perrett, T., Price, W., et al.: The epic-kitchens dataset: Collection, challenges and baselines. *IEEE Transactions on Pattern Analysis and Machine Intelligence* **43**(11), 4125–4141 (2020)
 15. Defays, D.: An efficient algorithm for a complete link method. *The Computer Journal* **20**(4), 364–366 (01 1977). <https://doi.org/10.1093/comjnl/20.4.364>, <https://doi.org/10.1093/comjnl/20.4.364>
 16. Deng, J., Dong, W., Socher, R., Li, L.J., Li, K., Fei-Fei, L.: Imagenet: A large-scale hierarchical image database. In: 2009 IEEE conference on computer vision and pattern recognition. pp. 248–255. Ieee (2009)
 17. Dong, S., Hu, H., Lian, D., Luo, W., Qian, Y., Gao, S.: Weakly supervised video representation learning with unaligned text for sequential videos. In: Proceedings of the IEEE/CVF Conference on Computer Vision and Pattern Recognition. pp. 2437–2447 (2023)
 18. Duong, H.T., Le, V.T., Hoang, V.T.: Deep learning-based anomaly detection in video surveillance: A survey. *Sensors* **23**(11) (2023). <https://doi.org/10.3390/s23115024>, <https://www.mdpi.com/1424-8220/23/11/5024>
 19. Fabian Caba Heilbron, Victor Escorcia, B.G., Niebles, J.C.: Activitynet: A large-scale video benchmark for human activity understanding. In: Proceedings of the IEEE Conference on Computer Vision and Pattern Recognition. pp. 961–970 (2015)
 20. Feichtenhofer, C.: X3d: Expanding architectures for efficient video recognition. In: Proceedings of the IEEE/CVF conference on computer vision and pattern recognition. pp. 203–213 (2020)
 21. Feichtenhofer, C., Fan, H., Malik, J., He, K.: Slowfast networks for video recognition. In: Proceedings of the IEEE/CVF international conference on computer vision. pp. 6202–6211 (2019)
 22. Forslund Jacobsen, M., Konge, L., Alberti, M., la Cour, M., Park, Y.S., Thomsen, A.S.S.: ROBOT-ASSISTED VITREORETINAL SURGERY IMPROVES SURGICAL ACCURACY COMPARED WITH MANUAL SURGERY: A randomized trial in a simulated setting. *Retina* **40**(11), 2091–2098 (Nov 2020)
 23. Furnari, A., Farinella, G.M.: What would you expect? anticipating egocentric actions with rolling-unrolling lstms and modality attention. In: Proceedings of the IEEE/CVF International Conference on Computer Vision. pp. 6252–6261 (2019)
 24. Ghamsarian, N., Taschwer, M., Putzgruber-Adamitsch, D., Sarny, S., El-Shabrawi, Y., Schoeffmann, K.: Lensid: A cnn-rnn-based framework towards lens irregularity detection in cataract surgery videos. In: de Bruijne, M., Cattin, P.C., Cotin, S., Padoy, N., Speidel, S., Zheng, Y., Essert, C. (eds.) *Medical Image Computing and Computer Assisted Intervention - MICCAI 2021 - 24th International Conference, Strasbourg, France, September 27 - October 1, 2021, Proceedings, Part VIII. Lecture Notes in Computer Science*, vol. 12908, pp. 76–86. Springer (2021). https://doi.org/10.1007/978-3-030-87237-3_8, https://doi.org/10.1007/978-3-030-87237-3_8
 25. Ghamsarian, N., Taschwer, M., Putzgruber-Adamitsch, D., Sarny, S., Schoeffmann, K.: Relevance detection in cataract surgery videos by spatio-temporal action localization. In: 25th International Conference on Pattern Recognition, ICPR 2020, Virtual Event / Milan, Italy, January 10-15, 2021. pp. 10720–10727. IEEE (2020). <https://doi.org/10.1109/ICPR48806.2021.9412525>, <https://doi.org/10.1109/ICPR48806.2021.9412525>

26. Grammatikopoulou, M., Flouty, E., Kadkhodamohammadi, A., Quellec, G., Chow, A., Nehme, J., Luengo, I., Stoyanov, D.: Cadis: Cataract dataset for image segmentation. arXiv preprint arXiv:1906.11586 (2019)
27. Gu, C., Sun, C., Ross, D.A., Vondrick, C., Pantofaru, C., Li, Y., Vijayanarasimhan, S., Toderici, G., Ricco, S., Sukthankar, R., Schmid, C., Malik, J.: Ava: A video dataset of spatio-temporally localized atomic visual actions (2018)
28. Gujjar, P., Vaughan, R.: Classifying pedestrian actions in advance using predicted video of urban driving scenes. In: 2019 International Conference on Robotics and Automation (ICRA). pp. 2097–2103 (2019). <https://doi.org/10.1109/ICRA.2019.8794278>
29. Horn, B.K., Schunck, B.G.: Determining optical flow. *Artificial intelligence* **17**(1-3), 185–203 (1981)
30. Ji, G.P., Xiao, G., Chou, Y.C., Fan, D.P., Zhao, K., Chen, G., Van Gool, L.: Video polyp segmentation: A deep learning perspective. *Machine Intelligence Research* **19**(6), 531–549 (Dec 2022). <https://doi.org/10.1007/s11633-022-1371-y>, <https://doi.org/10.1007/s11633-022-1371-y>
31. Jin, Y., Dou, Q., Chen, H., Yu, L., Qin, J., Fu, C.W., Heng, P.A.: SV-RCNet: Workflow recognition from surgical videos using recurrent convolutional network. *IEEE Trans. Med. Imaging* **37**(5), 1114–1126 (May 2018)
32. Kay, W., Carreira, J., Simonyan, K., Zhang, B., Hillier, C., Vijayanarasimhan, S., Viola, F., Green, T., Back, T., Natsev, P., et al.: The kinetics human action video dataset. arXiv preprint arXiv:1705.06950 (2017)
33. Kong, Y., Fu, Y.: Human action recognition and prediction: A survey. *International Journal of Computer Vision* **130**(5), 1366–1401 (May 2022). <https://doi.org/10.1007/s11263-022-01594-9>, <https://doi.org/10.1007/s11263-022-01594-9>
34. Kotseruba, I., Rasouli, A., Tsotsos, J.K.: Benchmark for Evaluating Pedestrian Action Prediction. In: Proceedings of the IEEE Winter Conference on Applications of Computer Vision (WACV). pp. 1258–1268 (2021)
35. Li, J., Jin, Y., Chen, Y., Yip, H.C., Scheppach, M., Chiu, P.W.Y., Yam, Y., Meng, H.M.L., Dou, Q.: Imitation learning from expert video data for dissection trajectory prediction in endoscopic surgical procedure. In: Greenspan, H., Madabhushi, A., Mousavi, P., Salcudean, S., Duncan, J., Syeda-Mahmood, T., Taylor, R. (eds.) *Medical Image Computing and Computer Assisted Intervention – MICCAI 2023*. pp. 494–504. Springer Nature Switzerland, Cham (2023)
36. Li, Y., Wu, C.Y., Fan, H., Mangalam, K., Xiong, B., Malik, J., Feichtenhofer, C.: Mvitv2: Improved multiscale vision transformers for classification and detection. In: Proceedings of the IEEE/CVF Conference on Computer Vision and Pattern Recognition. pp. 4804–4814 (2022)
37. Li, Y., Liu, M., Rehg, J.M.: In the eye of beholder: Joint learning of gaze and actions in first person video. In: Proceedings of the European conference on computer vision (ECCV). pp. 619–635 (2018)
38. Lin, S., Miao, A.J., Lu, J., Yu, S., Chiu, Z.Y., Richter, F., Yip, M.C.: Semantic-super: A semantic-aware surgical perception framework for endoscopic tissue identification, reconstruction, and tracking. In: 2023 IEEE International Conference on Robotics and Automation (ICRA). pp. 4739–4746 (2023). <https://doi.org/10.1109/ICRA48891.2023.10160746>
39. Lin, T., Liu, X., Li, X., Ding, E., Wen, S.: Bmn: Boundary-matching network for temporal action proposal generation. In: Proceedings of the IEEE/CVF international conference on computer vision. pp. 3889–3898 (2019)

40. Liu, B., Adeli, E., Cao, Z., Lee, K.H., Shenoi, A., Gaidon, A., Niebles, J.C.: Spatiotemporal relationship reasoning for pedestrian intent prediction. *IEEE Robotics and Automation Letters* **5**(2), 3485–3492 (2020)
41. Liu, Z., Ning, J., Cao, Y., Wei, Y., Zhang, Z., Lin, S., Hu, H.: Video swin transformer. arXiv preprint arXiv:2106.13230 (2021)
42. Long, F., Yao, T., Qiu, Z., Tian, X., Luo, J., Mei, T.: Bi-calibration networks for weakly-supervised video representation learning. *International Journal of Computer Vision* **131**(7), 1704–1721 (Jul 2023). <https://doi.org/10.1007/s11263-023-01779-w>, <https://doi.org/10.1007/s11263-023-01779-w>
43. Loukas, C.: Video content analysis of surgical procedures. *Surgical Endoscopy* **32**(2), 553–568 (Feb 2018). <https://doi.org/10.1007/s00464-017-5878-1>, <https://doi.org/10.1007/s00464-017-5878-1>
44. Lucas, B.D., Kanade, T., et al.: An iterative image registration technique with an application to stereo vision, vol. 81. Vancouver (1981)
45. Ma, Y., Chen, X., Cheng, K., Li, Y., Sun, B.: Ldpolypvideo benchmark: A large-scale colonoscopy video dataset of diverse polyps. In: de Bruijne, M., Cattin, P.C., Cotin, S., Padoy, N., Speidel, S., Zheng, Y., Essert, C. (eds.) *Medical Image Computing and Computer Assisted Intervention – MICCAI 2021*. pp. 387–396. Springer International Publishing, Cham (2021)
46. Maier-Hein, L., Wagner, M., Ross, T., Reinke, A., Bodenstedt, S., Full, P.M., Hempe, H., Mindroc-Filimon, D., Scholz, P., Tran, T.N., et al.: Heidelberg colorectal data set for surgical data science in the sensor operating room. *Scientific data* **8**(1), 101 (2021)
47. Mesejo, P., Pizarro, D., Abergel, A., Rouquette, O., Beorchia, S., Poincloux, L., Bartoli, A.: Computer-aided classification of gastrointestinal lesions in regular colonoscopy. *IEEE Transactions on Medical Imaging* **35**(9), 2051–2063 (2016). <https://doi.org/10.1109/TMI.2016.2547947>
48. Ming, H., Lin, W., Siyuan, Y., Don, M., Qingli, R., Peng, X., Wei, F., Peibo, D., Lie, J., Zongyuan, G.: Nurvid: A large expert-level video database for nursing procedure activity understanding. In: *Thirty-seventh Conference on Neural Information Processing Systems Datasets and Benchmarks Track* (2023)
49. Ni, B., Peng, H., Chen, M., Zhang, S., Meng, G., Fu, J., Xiang, S., Ling, H.: Expanding language-image pretrained models for general video recognition (2022)
50. Ni, Z.L., Bian, G.B., Zhou, X.H., Hou, Z.G., Xie, X.L., Wang, C., Zhou, Y.J., Li, R.Q., Li, Z.: Raunet: Residual attention u-net for semantic segmentation of cataract surgical instruments. In: *International Conference on Neural Information Processing (ICONIP)*. pp. 139–149. Springer (2019)
51. Nwoye, C.I., Gonzalez, C., Yu, T., Mascagni, P., Mutter, D., Marescaux, J., Padoy, N.: Recognition of instrument-tissue interactions in endoscopic videos via action triplets. In: *Medical Image Computing and Computer Assisted Intervention–MICCAI 2020: 23rd International Conference, Lima, Peru, October 4–8, 2020, Proceedings, Part III* 23. pp. 364–374. Springer (2020)
52. Nwoye, C.I., Padoy, N.: Data splits and metrics for benchmarking methods on surgical action triplet datasets. arXiv preprint arXiv:2204.05235 (2022)
53. Nwoye, C.I., Yu, T., Gonzalez, C., Seeliger, B., Mascagni, P., Mutter, D., Marescaux, J., Padoy, N.: Rendezvous: Attention mechanisms for the recognition of surgical action triplets in endoscopic videos. *Medical Image Analysis* **78**, 102433 (2022)
54. Pan, X., Gao, X., Wang, H., Zhang, W., Mu, Y., He, X.: Temporal-based swin transformer network for workflow recognition of surgical video. *Int. J. Comput. Assist. Radiol. Surg.* **18**(1), 139–147 (Jan 2023)

55. Park, J., Park, C.H.: Recognition and prediction of surgical actions based on online robotic tool detection. *IEEE Robotics and Automation Letters* **6**(2), 2365–2372 (2021)
56. Radford, A., Kim, J.W., Hallacy, C., Ramesh, A., Goh, G., Agarwal, S., Sastry, G., Askell, A., Mishkin, P., Clark, J., et al.: Learning transferable visual models from natural language supervision. In: *International conference on machine learning*. pp. 8748–8763. PMLR (2021)
57. Rasheed, H., khattak, M.U., Maaz, M., Khan, S., Khan, F.S.: Finetuned clip models are efficient video learners. In: *The IEEE/CVF Conference on Computer Vision and Pattern Recognition* (2023)
58. Ross, T., Reinke, A., Full, P.M., Wagner, M., Kenngott, H., Apitz, M., Hempe, H., Mindroc-Filimon, D., Scholz, P., Tran, T.N., et al.: Comparative validation of multi-instance instrument segmentation in endoscopy: results of the robust-mis 2019 challenge. *Medical image analysis* **70**, 101920 (2021)
59. Ross, T., Zimmerer, D., Vemuri, A., Isensee, F., Wiesenfarth, M., Bodenstedt, S., Both, F., Kessler, P., Wagner, M., Müller, B., et al.: Exploiting the potential of unlabeled endoscopic video data with self-supervised learning. *International journal of computer assisted radiology and surgery* **13**, 925–933 (2018)
60. Roy, D., Fernando, B.: Action anticipation using latent goal learning. In: *2022 IEEE/CVF Winter Conference on Applications of Computer Vision (WACV)*. pp. 808–816 (2022). <https://doi.org/10.1109/WACV51458.2022.00088>
61. Roß, T., Reinke, A., Full, P.M., Wagner, M., Kenngott, H., Apitz, M., Hempe, H., Mindroc-Filimon, D., Scholz, P., Tran, T.N., Bruno, P., Arbeláez, P., Bian, G.B., Bodenstedt, S., Bolmgren, J.L., Bravo-Sánchez, L., Chen, H.B., González, C., Guo, D., Halvorsen, P., Heng, P.A., Hosgor, E., Hou, Z.G., Isensee, F., Jha, D., Jiang, T., Jin, Y., Kirtac, K., Kletz, S., Leger, S., Li, Z., Maier-Hein, K.H., Ni, Z.L., Riegler, M.A., Schoeffmann, K., Shi, R., Speidel, S., Stenzel, M., Twick, I., Wang, G., Wang, J., Wang, L., Wang, L., Zhang, Y., Zhou, Y.J., Zhu, L., Wiesenfarth, M., Kopp-Schneider, A., Müller-Stich, B.P., Maier-Hein, L.: Comparative validation of multi-instance instrument segmentation in endoscopy: Results of the robust-mis 2019 challenge. *Medical Image Analysis* **70**, 101920 (2021). <https://doi.org/https://doi.org/10.1016/j.media.2020.101920>, <https://www.sciencedirect.com/science/article/pii/S136184152030284X>
62. Sato, F., Hachiuma, R., Sekii, T.: Prompt-guided zero-shot anomaly action recognition using pretrained deep skeleton features. In: *Proceedings of the IEEE/CVF Conference on Computer Vision and Pattern Recognition*. pp. 6471–6480 (2023)
63. Schoeffmann, K., Husslein, H., Kletz, S., Petscharnig, S., Münzer, B., Beecks, C.: Video retrieval in laparoscopic video recordings with dynamic content descriptors. *Multim. Tools Appl.* **77**(13), 16813–16832 (2018). <https://doi.org/10.1007/s11042-017-5252-2>, <https://doi.org/10.1007/s11042-017-5252-2>
64. Schoeffmann, K., Taschwer, M., Sarny, S., Münzer, B., Primus, M.J., Putzgruber, D.: Cataract-101: video dataset of 101 cataract surgeries. In: César, P., Zink, M., Murray, N. (eds.) *Proceedings of the 9th ACM Multimedia Systems Conference, MMSys 2018, Amsterdam, The Netherlands, June 12-15, 2018*. pp. 421–425. ACM (2018). <https://doi.org/10.1145/3204949.3208137>, <https://doi.org/10.1145/3204949.3208137>
65. Shi, D., Zhong, Y., Cao, Q., Ma, L., Li, J., Tao, D.: Tridet: Temporal action detection with relative boundary modeling. In: *Proceedings of the IEEE/CVF Conference on Computer Vision and Pattern Recognition*. pp. 18857–18866 (2023)

66. Shi, X., Jin, Y., Dou, Q., Heng, P.A.: LRTD: long-range temporal dependency based active learning for surgical workflow recognition. *Int. J. Comput. Assist. Radiol. Surg.* **15**(9), 1573–1584 (Sep 2020)
67. Sigurdsson, G.A., Varol, G., Wang, X., Farhadi, A., Laptev, I., Gupta, A.: Hollywood in homes: Crowdsourcing data collection for activity understanding. In: Leibe, B., Matas, J., Sebe, N., Welling, M. (eds.) *Computer Vision – ECCV 2016*. pp. 510–526. Springer International Publishing, Cham (2016)
68. Smedsrud, P.H., Thambawita, V., Hicks, S.A., Gjestang, H., Nedrejord, O.O., Næss, E., Borgli, H., Jha, D., Berstad, T.J.D., Eskeland, S.L., Lux, M., Espeland, H., Petlund, A., Nguyen, D.T.D., Garcia-Ceja, E., Johansen, D., Schmidt, P.T., Toth, E., Hammer, H.L., de Lange, T., Riegler, M.A., Halvorsen, P.: Kvasir-Capsule, a video capsule endoscopy dataset. *Scientific Data* **8**(1), 142 (2021). <https://doi.org/10.1038/s41597-021-00920-z>
69. Soomro, K., Zamir, A.R., Shah, M.: Ucf101: A dataset of 101 human actions classes from videos in the wild (2012)
70. Spaeth, G., Danesh-Meyer, H., Goldberg, I., Kampik, A.: *Ophthalmic Surgery: Principles and Practice E-Book*. Elsevier Health Sciences (2011), <https://books.google.com.hk/books?id=wHWMUGH-5csC>
71. Stauder, R., Ostler, D., Kranzfelder, M., Koller, S., Feußner, H., Navab, N.: The tum lapchole dataset for the m2cai 2016 workflow challenge. *arXiv preprint arXiv:1610.09278* (2016)
72. Suzuki, T., Kataoka, H., Aoki, Y., Satoh, Y.: Anticipating traffic accidents with adaptive loss and large-scale incident db. In: *Proceedings of the IEEE conference on computer vision and pattern recognition*. pp. 3521–3529 (2018)
73. Tian, Y., Pang, G., Liu, F., Liu, Y., Wang, C., Chen, Y., Verjans, J., Carneiro, G.: Contrastive transformer-based multiple instance learning for weakly supervised polyp frame detection. In: *International Conference on Medical Image Computing and Computer-Assisted Intervention*. pp. 88–98. Springer (2022)
74. Tran, D., Wang, H., Torresani, L., Feiszli, M.: Video classification with channel-separated convolutional networks (2019)
75. Twinanda, A.P., Shehata, S., Mutter, D., Marescaux, J., de Mathelin, M., Padoy, N.: Endonet: A deep architecture for recognition tasks on laparoscopic videos. *IEEE Transactions on Medical Imaging (TMI)* **36**, 86–97 (2016), <https://api.semanticscholar.org/CorpusID:5633749>
76. Twinanda, A.P., Yengera, G., Mutter, D., Marescaux, J., Padoy, N.: Rsdnet: Learning to predict remaining surgery duration from laparoscopic videos without manual annotations. *IEEE Transactions on Medical Imaging* **38**(4), 1069–1078 (2019). <https://doi.org/10.1109/TMI.2018.2878055>
77. Wagner, M., Müller-Stich, B.P., Kisilenko, A., Tran, D., Heger, P., Mündermann, L., Lubotsky, D.M., Müller, B., Davitashvili, T., Capek, M., et al.: Comparative validation of machine learning algorithms for surgical workflow and skill analysis with the heichole benchmark. *Medical Image Analysis* **86**, 102770 (2023)
78. Wang, T., Li, H., Pu, T., Yang, L.: Microsurgery robots: Applications, design, and development. *Sensors* **23**(20) (2023). <https://doi.org/10.3390/s23208503>, <https://www.mdpi.com/1424-8220/23/20/8503>
79. Wang, X., Zhang, S., Qing, Z., Shao, Y., Gao, C., Sang, N.: Self-supervised learning for semi-supervised temporal action proposal. In: *CVPR* (2021)
80. Wang, Z., Lu, B., Long, Y., Zhong, F., Cheung, T.H., Dou, Q., Liu, Y.: Autolaparo: A new dataset of integrated multi-tasks for image-guided surgical automation in laparoscopic hysterectomy. In: *International Conference on Medical Image Computing and Computer-Assisted Intervention*. pp. 486–496. Springer (2022)

81. Wu, W., Sun, Z., Ouyang, W.: Revisiting classifier: Transferring vision-language models for video recognition (2023)
82. Wu, W., Wang, X., Luo, H., Wang, J., Yang, Y., Ouyang, W.: Bidirectional cross-modal knowledge exploration for video recognition with pre-trained vision-language models. In: Proceedings of the IEEE/CVF Conference on Computer Vision and Pattern Recognition (2023)
83. Yengera, G., Mutter, D., Marescaux, J., Padoy, N.: Less is more: Surgical phase recognition with less annotations through self-supervised pre-training of cnn-lstm networks. arXiv preprint arXiv:1805.08569 (2018)
84. Yu, F., Silva Croso, G., Kim, T.S., Song, Z., Parker, F., Hager, G.D., Reiter, A., Vedula, S.S., Ali, H., Sikder, S.: Assessment of Automated Identification of Phases in Videos of Cataract Surgery Using Machine Learning and Deep Learning Techniques. *JAMA Network Open* **2**(4), e191860–e191860 (04 2019). <https://doi.org/10.1001/jamanetworkopen.2019.1860>, <https://doi.org/10.1001/jamanetworkopen.2019.1860>
85. Yu, T., Mutter, D., Marescaux, J., Padoy, N.: Learning from a tiny dataset of manual annotations: a teacher/student approach for surgical phase recognition. arXiv preprint arXiv:1812.00033 (2018)
86. Zha, R., Cheng, X., Li, H., Harandi, M., Ge, Z.: Endosurf: Neural surface reconstruction of deformable tissues with stereo endoscope videos. In: International Conference on Medical Image Computing and Computer-Assisted Intervention. pp. 13–23. Springer (2023)
87. Zhang, C.L., Wu, J., Li, Y.: Actionformer: Localizing moments of actions with transformers. In: European Conference on Computer Vision. LNCS, vol. 13664, pp. 492–510 (2022)
88. Zhang, C., Wu, J., Li, Y.: Actionformer: Localizing moments of actions with transformers. In: European Conference on Computer Vision (2022)
89. Zhao, H., Wildes, R.P.: On diverse asynchronous activity anticipation. In: Vedaldi, A., Bischof, H., Brox, T., Frahm, J.M. (eds.) *Computer Vision – ECCV 2020*. pp. 781–799. Springer International Publishing, Cham (2020)
90. Zhou, L., Xu, C., Corso, J.J.: Towards automatic learning of procedures from web instructional videos. In: *AAAI Conference on Artificial Intelligence*. pp. 7590–7598 (2018), <https://www.aaai.org/ocs/index.php/AAAI/AAAI18/paper/view/17344>

7 Training Details

We conducted all experiments using 4 NVIDIA RTX3090Ti GPUs.

7.1 Training Details for Classification Tasks

We employed the officially released codes to train all recognition models. The SlowFast [21], I3D [11] and X3D [20] models were trained for 150 epochs with a batch size of 16, using a base learning rate of 0.001. We employed a cosine decay learning rate scheduler with 34 warmup epochs. We sampled 16 frames per clip with a sampling rate of 16. For the configuration of training MViT v2 [36] model, we apply the base learning 0.0001, cosine decay learning rate scheduler, 200 training epochs, 30 warmup epochs, and the batch size 8. We sample 16 frames per clip with the sampling rate of 16.

7.2 Training Details for Localization Task

Feature extraction. We firstly extract the frames from each video with 25 FPS and also extract the optical flow with TV-L1 [29,44] algorithm. After that, we finetune an I3D [11] model on Kinetics 400 [32], and then use it to generate the features for each RGB and optical flow frame. Since each video has variable duration, we perform the uniform interpolation to generate 100 fixed-length features for each video. Finally, we concatenate the RGB and optical flow features into a 2048-dimensional embedding as the model input.

Model training. We train all the detection models with their officially released code and the default configurations. For training ActionFormer [88] model, we apply the base learning rate 0.001, cosine decay learning rate scheduler, 30 training epochs, 5 warmup epochs, and the batch size 16. For training TriDet [65] model, we apply the base learning rate of 0.0004, step decay learning rate scheduler, 20 training epochs, and the batch size 200. For these two baseline models, we employed three different backbone network settings for performance comparison: CSN [74], SwinVivIT [41], and SlowFast [21].

7.3 Training Details for Anticipation Task

We follow the same settings as used in classification experiment.

8 Annotation Interface Demonstration

8.1 Video Filtering

The videos in the OphNet dataset, sourced from YouTube, exhibit a variety of styles, resolutions, and on-screen elements. To ensure quality and relevance, we filtered out videos that do not provide a microscopic perspective (first row of Fig. 5), as well as those with subtitles, additional video windows, or watermarks

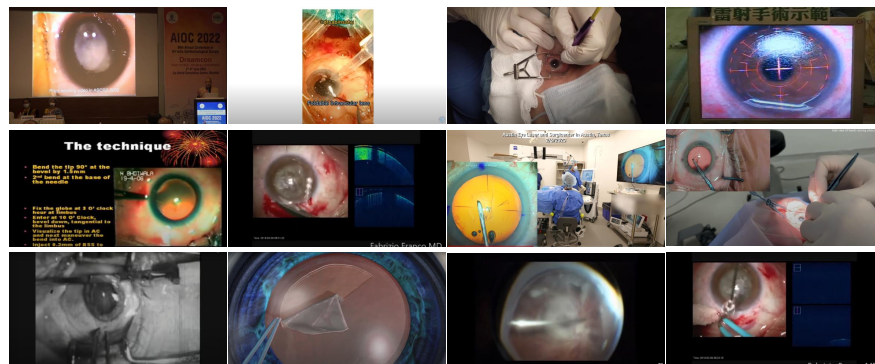


Fig. 5: Examples of filtered videos.



Fig. 6: Examples with minor flaws that were still retained.

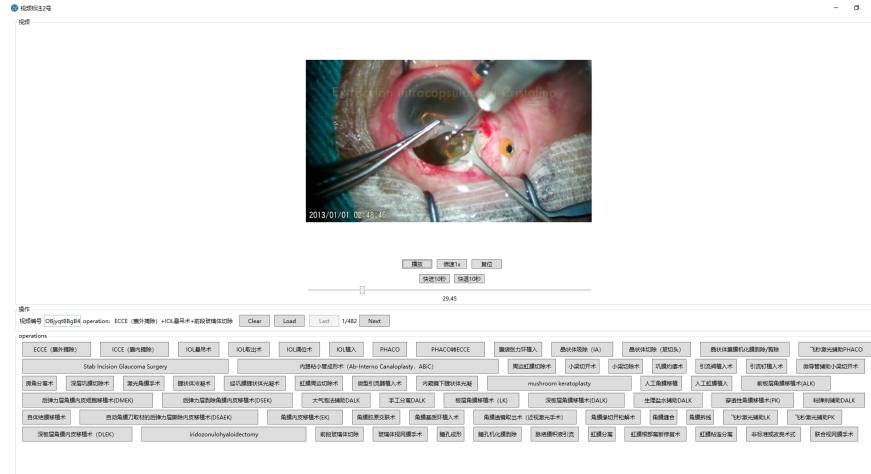
occupying a significant portion of the frame (second row of Fig. 5). Furthermore, videos depicting unrealistic animations, suffering from poor resolution, displaying grayscale images, or containing OCT imagery (third row of Fig. 5) were also excluded. However, we retained videos with minimal on-screen text or watermarks (first row of Fig. 6). Additionally, 3D videos recorded using binocular microscopes were preserved, albeit processed to retain only the left-eye perspective in our dataset.

8.2 Classification Annotation Interface

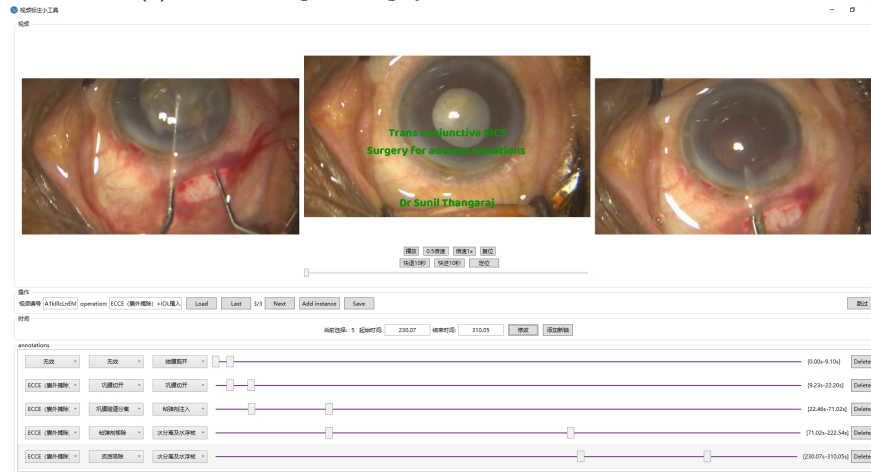
In this stage, we categorize the videos into valid and invalid videos through keypresses, with valid videos further classified based on their primary surgical type. Initially, an attending ophthalmologist categorizes the videos into three types: cataract surgery, glaucoma surgery, and corneal surgery. These are then further distributed for filtering and classification annotation, with each individual responsible for one of the three major surgeries.

8.3 Hierarchical Localization Annotation Interface

We have designed an interface that supports three levels of annotation: surgery, phase, and operation, and is easy to operate and modify later. The main window



(a) Video filtering and surgery classification annotation interface.



(b) Hierarchical temporal localization annotation interface for surgery, phase, and operation

Fig. 7: Annotation Interface Design

plays the video (with features such as speed adjustment, fast forward, rewind, and pause), while the left and right sub-windows display the corresponding frames for the start and end times of the current annotated segment. Additionally, it supports functions such as automatic time positioning and instance insertion.

9 Dataset Bias

Dataset Bias. OphNet’s videos are sourced from YouTube and exhibit diverse styles, clarity, and screen elements. This diversity can aid detection models in generalization but may affect their effectiveness and performance. Some videos in the dataset include subtitles or additional video windows, such as watermark

shown in Fig. 5. Similarly, additional video windows offer another perspective but can make the scene chaotic, making it harder to recognize primary surgical actions. The presence of these factors in OphNet reflects the complexity of real-world surgical environments, because an ophthalmic microscope may inherently display different windows or show parameters during recording. While they pose challenges, they also present opportunities for developing models that can better handle variability and unpredictability, which are crucial aspects of real-world surgical scenarios.

Annotation Bias. OphNet is entirely annotated by ophthalmologists, and while this ensures a high level of expertise, it also introduces the possibility of annotation bias reflecting specific regional practices, terminologies, and interpretations. Despite the universal nature of many ophthalmic procedures, subtle differences in surgical techniques, procedural preferences, and clinical terminologies could lead to inconsistencies in how surgeries are categorized and described across different regions. For instance, the technique for cataract extraction may vary between phacoemulsification in one region and manual small incision cataract surgery in another, leading to differences in the annotation of surgical phases and operations. Similarly, the terminology used to describe certain procedures might differ, with one region referring to a procedure as "anterior vitrectomy" while another uses "pars plana vitrectomy." To reduce the possibility of biases in precise annotations, we have taken great care to establish a unified definition prior to describing the surgery, phase, and operation. However, potential biases arising from regional variations and individual surgical practices are inevitable. Recognizing these potential biases is crucial for the users of OphNet, as it allows for a more nuanced interpretation of the data and its applicability to different clinical settings. Future work could involve expanding the annotation team to include ophthalmologists from diverse geographical regions and surgical backgrounds, further mitigating the impact of regional and individual biases on the dataset.

10 OphNet’s Extension

Multi-Surgery Recognition. In the realm of surgical procedures, obtaining large-scale, finely annotated video datasets is a formidable challenge due to privacy concerns, the extensive time required for detailed labeling by medical experts, and the complexity of surgical actions. Consequently, weak supervision emerges as a pivotal approach, enabling the utilization of limited or imprecise labels to train robust models capable of understanding and recognizing diverse surgical activities. Looking forward, the integration of domain knowledge, such as surgical ontologies and procedural guidelines, into learning frameworks holds the potential to mitigate the limitations posed by weak labels. Additionally, the exploration of unsupervised and semi-supervised methods, combined with weak supervision, could provide new pathways for leveraging unlabelled video data effectively. Collaboration between computer scientists, clinicians, and domain

experts is essential to develop more sophisticated algorithms that can understand and predict surgical dynamics accurately.

Few-shot Learning. Few-shot learning approaches aim to develop models that can generalize from very limited labeled data, a scenario commonly encountered in the medical field due to the high cost, privacy issues, and time constraints associated with annotating surgical videos. In the context of surgery, these methods are particularly valuable as they allow for the recognition and understanding of surgical actions, tools, and phases from only a handful of examples, thereby facilitating broader applicability across diverse surgical procedures and settings.

Domain Generalization. Domain Generalization (DG) techniques are increasingly vital as they allow models to be robust and applicable across different hospitals, surgical procedures, and patient demographics, without the need for retraining. This is particularly crucial in surgical video analysis, where the variance in lighting, surgical techniques, equipment, and individual patient anatomy can vastly differ.